Accepted Manuscript

Electrochemiluminescence Resonance Energy Transfer Between Graphene Quantum Dots and Graphene Oxide for Sensitive Protein Kinase Activity and Inhibitor Sensing

Ru-Ping Liang, Wei-Bin Qiu, Hui-Fang Zhao, Cai-Yun Xiang, Jian-Ding Qiu

PII: S0003-2670(15)01416-6

DOI: 10.1016/j.aca.2015.11.034

Reference: ACA 234273

To appear in: *Analytica Chimica Acta*

Received Date: 5 June 2015

Revised Date: 30 October 2015

Accepted Date: 23 November 2015

Please cite this article as: R.-P. Liang, W.-B. Qiu, H.-F. Zhao, C.-Y. Xiang, J.-D. Qiu, Electrochemiluminescence Resonance Energy Transfer Between Graphene Quantum Dots and Graphene Oxide for Sensitive Protein Kinase Activity and Inhibitor Sensing, *Analytica Chimica Acta* (2016), doi: 10.1016/j.aca.2015.11.034.

Graphical Abstract

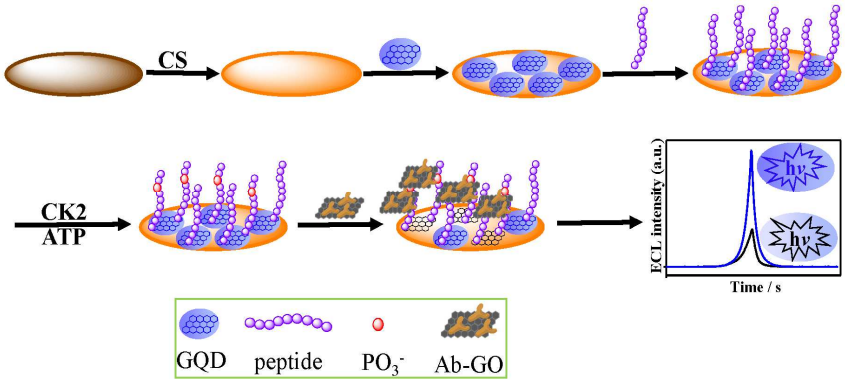

Electrochemiluminescence Resonance Energy Transfer Between Graphene Quantum Dots and Graphene Oxide for Sensitive Protein Kinase Activity and Inhibitor Sensing

Ru-Ping Liang, Wei-Bin Qiu, Hui-Fang Zhao, Cai-Yun Xiang, Jian-Ding Qiu*

Department of Chemistry, Nanchang University, Nanchang 330031, PR China

*Corresponding author. Tel.: +86 791 83969518.

E-mail address: jdqiu@ncu.edu.cn (J.-D. Qiu).

ABSTRACT

Herein, a novel electrochemiluminescence resonance energy transfer (ECL-RET) biosensor using graphene quantum dots (GQDs) as donor and graphene oxide (GO) as acceptor for monitoring the activity of protein kinase was presented for the first time. Anti-phosphoserine antibody conjugated graphene oxide (Ab-GO) nonocomposite could be captured onto the phosphorylated peptide/GQDs modified electrode surface through antibody-antigen interaction in the presence of casein kinase II (CK2) and adenosine 5′-triphosphate (ATP), resulting in ECL from the GQDs quenching by closely contacting GO. This ECL quenching degree was positively correlated with CK2 activity. Therefore, on the basis of ECL-RET between GQDs and GO, the activity of protein kinase can be detected sensitively. This biosensor can also be used for quantitative analysis CK2 activity in serum samples and qualitative screening kinase inhibition, indicating the potential application of the developed method in biochemical fundamental research and clinical diagnosis.

Keywords: Electrochemiluminescence resonance energy transfer; Graphene quantum dots; Casein kinase II activity; Graphene oxide.

1. Introduction

Protein kinases can catalyze the phosphorylation of proteins by transferring phosphate groups from adenosine 5′-triphosphate to the OH group of an amino acid side chain in peptides or proteins and generate adenosine diphosphate in the process. Protein kinases make up a huge super family of enzymes (termed the "kinome") and play a critical regulatory role in many fundamental biological processes [1]. With more than 300 protein substrates identified to date, the Ser/Thr-specific protein kinase-casein kinase II (CK2) is probably the most pleiotropic member of the human kinome. Abnormal expression of casein kinase has been implicated in a number of diseases including cancers, HIV and Alzheimer's disease [2-4]. The identification of kinase activities and their potential inhibitors is not only essential for basic biology to clarify molecular mechanisms of signal transduction, but also valuable for kinase-targeted drug discovery. The methods for the measurement of protein kinase activities include isotope labeling technique [5,6], mass spectroscopy [7], electrochemistry [8], and magnetic resonance imaging [9]. Although these methods all have their own advantages, most of them suffer from the drawbacks such as harmful radioactive labels, specialized/sophisticated instrumentation, complicated sample handling, or tedious operations [10]. Therefore, the development of sensitive, reliable, and cost-effective protein kinase assays for disease diagnosis and high-throughput screening of kinase inhibitors still remains a great challenge.

Resonance energy transfer (RET) between molecules, which plays a central role in many areas of modern chemistry and physics, is recognized as a sensitive and reliable analytical technique dependent on the spectral overlap between energy donor and acceptor as well as their

separation [11]. In recent years, RET systems based on the varied forms of luminescence have been developed for the assay of protein, immunoassay, and biosensing [12-14]. Clegg summed up fluorescence resonance energy transfer (FRET) approach for proteins and nucleic acids assays [15]. Recently, biosensor based on FRET from CdSe/ZnS quantum dots (QDs) to fluorophore for CK2 assay has been developed [16]. Although good results were obtained, it suffered from the strong background autofluorescence caused by the external illumination. Electrochemiluminescence resonance energy transfer (ECL-RET), which occurred based on the overlap of the ECL spectrum of the ECL species with the absorption spectrum of the acceptor, was a promising approach for further study of energy transfer. Due to the advantage of the absence of background arising from nonselective photoexcitation, high sensitivity, wide dynamic concentration response range, and so on [17], the ECL-RET assays have been used for DNA detection [18,19], cytosensing [20,21], and immunoassay [22]. However, the inherent toxicity of Cd-based semiconductors used in most ECL-RET studies may raise serious health and environmental problems [23]. Therefore, the search for benign nanomaterials with strong and stable ECL emission as donor has become an urgent challenge.

Graphene quantum dots (GQDs), the recently emerging carbon-based materials, are graphene sheets smaller than 100 nm. Due to the low cytotoxicity and attractive biocompatibility, it is of considerable interest to study the ECL behaviors of GQDs. Up to now, few studies have been found involving the ECL research of GQDs. Zhu et al. synthesized two-color GQDs and applied them for detection of Cd^{2+} in ECL biosensing [23]. Qiu et al. developed an Au NPs mediated dual-potential ECL ratiometric sensing approach for protein kinase A analysis using

GQDs and luminol as emitters [24]. Lu and co-workers reported the biosensor based on the ECL-RET between GQDs and Au NPs in solution for detection of p53 ssDNA [25]. Graphene, a two-dimensional carbon crystal with only one atom thickness, can act as an excellent energy acceptor due to its extraordinary electronic properties [26]. Dong et al. designed a novel biosensor for effective detection of target DNA by FRET from CdTe QDs to graphene oxide (GO) [27]. Zhao et al. proposed a universal immunosensing strategy based on interaction between graphene and GQDs for sensitive detection of human immunoglobulin G [28]. Owing to the similar nature of the QD-based ECL emission and photoluminescence, energy transfer between QD and GO has been considered for the design of new QD-based ECL analytical methodologies [29]. However, no references have been found that both GQDs as the donor and GO as the acceptor are integrated into one system for ECL-RET bioanalysis.

In this work, a novel ECL-RET system using GQDs as donor and GO as acceptor was designed for monitoring the activity of protein kinase (Scheme 1). Using CK2 as a model, the biosensor was fabricated by covalent binding GQDs onto chitosan film electrode and then functionalized with peptides through the amide reaction to form peptide/GQDs modified electrode. In the presence of CK2 and adenosine 5′-triphosphate, the peptides were phosphorylated, and then anti-phosphoserine antibody conjugated graphene nanocomposite was captured onto the phosphorylated peptide/GQDs electrode surface, resulting in high ECL quenching of GQDs. This ECL quenching degree was positively correlated with CK2 activity. To the best of our knowledge, it is the first time to profile the kinase activity based on ECL-RET mechanism using GQDs as donor and GO as acceptor, respectively. Thus, sensitive kinase

activity assay and quantitative kinase inhibitor screening can be achieved using this strategy.

Scheme 1

2. Experimental

2.1. Materials and Reagents, Apparatus, Synthesis of Graphene Oxide Sheets and GQDs, and Preparation of Ab-GO Bioconjugates were presented in Supplementary Material.

2.2. Preparation of the Biosensor

The glassy carbon electrode (GCE) was polished with 1.0, 0.3, and 0.05 μm α-Al_2O_3 powder on fine abrasive paper and then rinsed with ethanol and water. After the electrode was rinsed thoroughly with ultrapure water and allowed to dry with N_2 at room temperature, 10 μL chitosan (CS) solution (0.5% w/w) was dropped on the GCE surface and dried in air. The resulting CS/GCE was then immersed in a solution containing 0.1 mg/mL carboxylated GQDs and 5 mM EDC for 5 h at room temperature to obtain GQDs/CS/GCE. After rinsing with 0.1 M pH 7.4 PBS, the electrode was dipped into a solution containing 5 mM EDC, 8 mM NHS, and 50 μM peptide at room temperature in darkness for 8 h to yield peptide/GQDs/CS/GCE. CK2-catalyzed phosphorylation reaction was performed by placing the modified electrode in an assay buffer solution (20 mM Tris-HCl and 20 mM $MgCl_2$, pH 7.4) containing a desired amount of CK2 and ATP at 37 °C for 2 h. The phosphorylated peptide modified electrode was obtained. For CK2 inhibitor assay, the procedures were similar as above, except that different concentrations of inhibitor were added in the CK2 reaction mixture.

2.3. ECL Characterization and Kinase Activity Detection

The phosphorylated peptide modified electrode was immersed into a monoclonal anti-phosphoserine antibody conjugated graphene nanocomposite (Ab-GO) solution at 25 °C for 1 h to capture Ab-GO onto the phosphorylated peptide/GQDs/CS/GCE surface due to the specific antibody-antigen interaction. After being washed to remove the nonspecific adsorption, the resulting electrode was characterized by an ECL technique in 0.1 M pH 7.4 PBS buffer solution containing 0.1 M $K_2S_2O_8$ and 0.1 M KCl, the potential range was set from -1.6 to 0 V.

3. Results and discussion

3.1. Characterization of GO and GQDs

The morphology, structure and optical properties of GQDs were examined by transmission electron microscopy (TEM), Fourier transform infrared (FTIR), UV-vis absorption, and photoluminescence (PL) spectra. The TEM image of GO displayed a uniform structure, which appeared transparent and was folded over on one edge with isolated small fragments of graphene on its surface (Fig. 1A). After hydrothermal treatment of graphene sheets [30], the formed GQDs were dispersed with an average diameter of ca. 8 nm (Fig. 1B), confirming the successful synthesis of high crystallized GQDs [31,32]. For the FTIR spectrum of GQDs (Fig. 1C, curve a), the vibrational absorption band associated with the stretching of C-OH at 1240 cm^{-1} and C-O-C groups at 1052 cm^{-1} became weaker after the hydrothermal reduction. After chloroacetic acid activation, the resulting GQDs derivative showed stronger absorption bands at 1725 cm^{-1}, 1240 cm^{-1} and 1052 cm^{-1} (Fig. 1C, curve b), indicating the formation of carboxylated GQDs. To further explore the optical properties of the GQDs and mechanism of PL quenching between the GQDs and GO, UV−vis absorption and PL spectroscopic characterizations were collected (Fig.

1D). GO (curve a) displayed a maximum absorption at 229 nm due to the π-π* transition of aromatic C=C bonds and a shoulder around 300 nm due to the n-π* transition of C=O bonds [27,33]. Upon excitation with 310 nm beam, the PL spectra of the GQDs (curve b) and carboxylated GQDs (curve c) showed strong peaks at 445 nm with a stokes shift of 135 nm. Obviously, the PL emission of the GQDs had a considerable spectral overlap with absorption of GO, which was necessary for efficient energy transfer in photoluminescence or chemiluminescence system. In addition, it was clear that the GQDs were homogeneous and yellow color under daylight (picture 1) and exhibited blue photoluminescence under irradiation by a 365 nm UV light (picture 2). No distinct color changed in carboxylated GQDs under daylight (picture 3) and 365 nm UV light (picture 4) were observed, indicating that nearly no change in optical properties of GQDs and carboxylated GQDs occurred. Based on this necessary overlap for efficient energy transfer in a photoluminescence or chemiluminescence system, the successful ECL energy transfer between GQDs and GO could be achieved.

Figure 1

3.2. Characterization of the Biosensor

The stepwise reactions on the electrode surface are confirmed by electrochemical impedance spectroscopy (EIS). The semicircle portion observes at high frequencies corresponds to the electron-transfer limited process (Ret), a line portion observes at low frequencies by diffusion process [34]. As shown in Fig. 2, the bare GCE revealed a small semicircle domain (curve a), which implied a low Ret value of the redox couple of $Fe(CN)_6^{3-/4-}$. Due to its nonconductive

properties, CS film could inhibit the electron transfer, leading to increased Ret for the redox probe (curve b). Upon immobilizing carboxylated GQDs (simply GQDs for short) on the CS modified electrode, Ret remarkably increased (curve c) due to the fact that carboxylated GQDs carried more negative charges [35]. The Ret increased further after the assembly of peptide (curve d). After the phosphorylation of peptides by 5 U/mL CK2 and 50 μM ATP, the resulting phosphorylated peptide/GQDs/CS modified electrode showed a much higher resistance (curve e), indicating that phosphate groups had been transferred from ATP to peptides under the catalyzation of CK2. When assembling of Ab-GO on the electrode surface through the specific immunoreaction between phosphorylated peptide on phosphorylated peptide/GQDs/CS modified electrode surface and anti-phosphoserine antibody conjugated on Ab-GO nanocomposite, the Ret increased obviously (curve f), the reason could be attributed to that the formed immunocomplex on the electrode surface acted as the inert electron and mass-transfer blocking layer which further hindered the electron-transfer of $Fe(CN)_6^{3-/4-}$. To give more detailed information about the impedance of the modified electrode, a modified Randle-sequivalent circuit (inset in Fig. 2) was chosen to fit the measured results. All these experimental results demonstrate the sensing interface has been successfully fabricated according to Scheme 1.

Figure 2

The atomic force microscopy (AFM) technique was employed to characterize the assembling processes of the biosensor. AFM image of CS film appeared a little undulate height less than 1 nm (Fig. 3A). After the modification of GQDs, plenty of dots with a height of ca. 2.0 nm were

presented (Fig. 3B), suggesting that GQDs was successfully assembled onto CS film through the amide reaction. After peptide was covalently bound to the GQDs/CS surface, larger light dots were observed and the height increased to ca. 6 nm (Fig. 3C). When Ab-GO was assembled on the phosphorylated peptide/GQDs/CS surface, a large number of prominences with the height of ca. 21 nm appeared obviously (Fig. 3D), which was consistent with the size of the Ab-GO bioconjugates (Fig. S1 in the Supplementary Materials), demonstrating the successful capture of the Ab-GO bioconjugates on the phosphorylated peptide/GQDs/CS surface. The results demonstrate that the assembling processes of the biosensor can be realized according to Scheme 1.

Figure 3

3.3. ECL Behavior of the Biosensor

To demonstrate the feasibility of the developed biosensor, ECL response of the different modified electrodes was investigated in 0.1 M pH 7.4 PBS containing 0.1 M $K_2S_2O_8$ and 0.1 M KCl (Fig. 4). The ECL-voltage curves of the bare GCE (curve a) and CS/GCE (curve b) showed neglectable ECL emission, indicating the background ECL signal of the electrodes was very low. After conjugating GQDs on CS modified electrode surface, the cathodic ECL signal appeared obviously (curve c), demonstrating the strong ECL behavior of GQDs. When peptides were covalently conjugated to the GQDs/CS electrode surface, the ECL signal of the immobilized GQDs slightly decreased (curve d), due to the increased electron-transfer resistance and the inhibition of the peptide to the reaction between $K_2S_2O_8$ and GQDs. A little decrease of the ECL

signal was observed after assembly of Ab-GO onto the peptide/GQDs/CS modified electrode surface in the presence of 0 U/mL CK2 and 50 μM ATP (curve e), due to the slight nonspecific binding interaction between the peptide and GO. While the ECL signal decreased distinctly after the Ab-GO was assembled onto the phosphorylated peptide/GQDs/CS modified electrode surface in the presence of 5 U/mL CK2 and 50 μM ATP (curve f), demonstrating the successful fabrication of the ECL-RET sensing platform for kinase activity monitoring. The possible mechanism of the ECL reaction of GQDs is described as follow [23].

$$GQDs + ne^- \rightarrow nGQDs^{\bullet -}$$
$$S_2O_8^{2-} + e^- \rightarrow S_2O_8^{\bullet 2-}$$
$$S_2O_8^{\bullet 2-} \rightarrow SO_4^{2-} + SO_4^{\bullet -}$$
$$GQDs^{\bullet -} + SO_4^{\bullet -} \rightarrow GQDs^* + SO_4^{2-}$$
$$GQDs^* \rightarrow GQDs + hv$$

According to the mechanisms, strongly oxidizing $SO_4^{\bullet -}$ radicals and $GQDs^{\bullet -}$ radicals were produced by electrochemical reduction of $S_2O_8^{2-}$ and GQDs, respectively. Then, $SO_4^{\bullet -}$ radicals reacted with $GQDs^{\bullet -}$ via electron-transfer annihilation, producing excited state $GQDs^*$ which finally emitted light. In the fixed amount of $S_2O_8^{2-}$, the cathodic ECL intensity at -1.20 V depended on the concentration of the $GQDs^*$. When the Ab-GO was assembled on the phosphorylated peptide/GQDs/CS film surface through the antibody-antigen interaction, the GO was close to GQDs at short proximity, which could induce the energy transfer from GQDs to GO, resulting in a decrease of the excited state $GQDs^*$, and thereby the decrease of the cathodic ECL intensity. At higher kinase activity, more Ab-GO would be captured onto the electrode surface, giving better ECL-RET with GQDs. On the basis of the decreased cathodic ECL signal from the

ECL-RET between GQDs and GO, kinase activity can be determined indirectly.

Figure 4

3.4. ECL Measurement of CK2 Activity

The analytical performance of the ECL biosensor was characterized under optimal experimental conditions (Fig. S2 in the Supplementary Materials). As shown in Fig. 5A, with increasing CK2 concentration, the cathodic ECL signal from GQDs decreased correspondingly. The decreased ECL intensity linearly depended on the CK2 concentration in the range from 0.05 to 5 U/mL with the detection limit of 0.023 U/mL (S/N = 3) (Fig. 5B). The detection range of the method was much wider than those of previously reported 0–0.5 U/mL on an electrochemical strategy using TiO_2/MWNTs nanocomposites [36], 0.1–1.0 U/mL on a photoluminescence assay using GQDs as optical probe [32], and 0.08–2.0 U/mL on a fluorescent assay using peptide biomineralized gold nanoclusters as signal sensing probe [37]. The detection limit was much lower than those of 0.1 U/mL on a FRET-based method [16], and 0.03 U/mL on a photoluminescence assay using GQDs as probe [32]. The decreased ECL intensity as a function of CK2 concentration confirmed our speculation that the high quenching efficiency of GO to the ECL of GQDs led to high sensitivity for ECL-RET-based biosensing of CK2. These results demonstrate that the proposed ECL-RET-based strategy can be employed for highly sensitive kinase activity detection in a wide concentration range.

Figure 5

3.5. Kinase Activity Inhibition Evaluation

This proposed strategy for the detection of kinase activity was further employed to quantitatively characterize the inhibition of CK2 activity. Ellagic acid, which possesses anti-mutagenic and anti-carcinogenic properties as a potent and cell-permeable antioxidant [38], was employed as the model inhibitor in this research. As shown in Fig. 6A, the ECL signal from GQDs increased with increasing concentration of ellagic acid, and then reached a stable level when the concentration of ellagic acid was over 0.15 μM. The ECL intensity and different concentrations of the ellagic acid curves were supplied in the inset of Fig. 6A. From which the IC_{50} value (inhibitor concentration producing 50% inhibition) for ellagic acid was estimated to be 0.043 μM, which was well comparable with that reported in the literature [38]. To further demonstrate the potential of this strategy for screening kinase inhibitors, the inhibition of CK2 phosphorylation activity by other three different inhibitors such as quercetin, emodin, and 5,6-dichlorobenzimidazole-l-β-D-ribofuranoside (DRB), was also tested by comparing ECL signal from samples incubated with inhibitors against that without any inhibitor. Different ECL intensities in the presence of the same concentration of inhibitors were shown in Fig. 6B. Quercetin and emodin could strongly inhibit the CK2 activity, while DRB was a relatively weaker inhibitor, and the inhibition efficiency of ellagic acid was the most serious one, in good agreement with the order obtained in previous reports [39]. Therefore, the above results demonstrate that our method can be successfully used in the assay of CK2 inhibitors and the qualitative screening of kinase inhibitors.

Figure 6

3.6. Specificity of ECL Biosensor

To evaluate the specificity of the assay, different proteins or enzymes, such as bovine serum albumin (BSA), glucose oxidase (GOx), and alcohol dehydrogenase (ADH), were tested (Fig. S3). In comparison with that in the case of CK2, only slight ECL intensity change was attained for BSA, GOx, and ADH. These results suggest that the proposed method possesses high selectivity to CK2 assay.

3.7. Reproducibility and Precision of ECL Biosensor

ECL emission of the biosensor at CK2 concentration of 2.5 U/mL under continuous potential scans in a 0.1 M PBS containing 0.1 M $K_2S_2O_8$ and 0.1 M KCl was shown in Fig. S4. Strong and stable ECL signals were observed with a relative standard deviation of 0.97%, which signified that the ECL biosensor possessed excellent potential cycling stability. The reproducibility of the ECL biosensor was also studied with intra-and inter-assay precision. The intra-assay precision of the ECL biosensor was evaluated by measuring the 2.5 U/mL of CK2 activity ten times. The inter-assay precision was assessed by assaying the same level of CK2 activity with ten electrodes. The intra- and the inter-assay variation coefficients obtained from 2.5 U/mL CK2 were 6.7% and 8.1%, respectively, giving acceptable repeatability and fabrication reproducibility. When the biosensor was not in use, it was stored in air condition at 4 °C. No obvious change in the ECL intensity of GQDs was observed after storage for 4 weeks, exhibiting a potential application in practice.

3.8. CK2 Activity Assay in Complex Biological Samples

To further investigate the proposed ECL-RET-based assay in complex biological samples for

clinic application, the phosphorylation reaction solution was prepared by adding a desired amount of CK2 in human serum rather than buffer solution. As shown in Table S1 in the Supplementary Materials, the recoveries were in the range of 97–103% for measurement of 0.1, 1.0 and 2.5 U/mL CK2 spiked in serum with a maximum RSD of 3.0%, suggesting that the as-proposed ECL assay holds a great promise in practical applications for CK2 detection with great accuracy and reliability.

4. Conclusion

In conclusion, a novel signal-off sensing platform for sensitive detection of CK2 activity based on the ECL-RET between GQDs and GO was proposed for the first time. The GO was acted as the acceptor to quench the cathodic ECL of GQDs, resulting in a new ECL-RET sensing approach for CK2 detection. At a higher concentration of kinase, the more Ab-GO could be effectively captured onto the phosphorylated peptide/GQDsmodified electrode surface, giving more ECL-RET between GQDs and GO. The ECL quenching degree was positively correlated with CK2 activity. As a result, the as-proposed ECL-RET-based biosensor offered a highly sensitive strategy for CK2 activity monitoring with a low detection limit, wide linear range, and good stability. Moreover, the proof-of-concept method also showed excellent performance on the accurate and quantitative kinase inhibitor assay, verifying with well-known kinase inhibition systems. It is expected that the novel strategy will open new opportunities for development of the ECL-RET technique and promote the applications of carbon-based nanomaterials in bioassays.

Acknowledgements

We greatly appreciate the supports of the National Natural Science Foundation of China (Nos.

21163014, 21265017 and 21475056) and the Program for New Century Excellent Talents in University (Nos. NCET-11-1002 and NCET-13-0848).

References

[1] G. Manning, D. B. Whyte, R. Martinez, T. Hunter, S. Sudarsanam, Science 298 (2002) 1912-1934.

[2] H. Wang, A. Davis, S. Yu, K. Ahmed, Mol. Cell. Biochem. 227 (2001) 167-174.

[3] J. W. Critchfield, J. E. Coligan, T. M. Folks, S. T. Butera, Proc. Natl. Acad. Sci. U. S. A. 94 (1997) 6110-6115.

[4] M. Flajolet, G. He, M. Heiman, A. Lin, A. C. Nairn, P. Greengard, Proc. Natl. Acad. Sci. U. S. A. 104 (2007) 4159-4164.

[5] B. T. Houseman, J. H. Huh, S. J. Kron, M. Mrksich, Nat. Biotechnol. 20 (2002) 270-274.

[6] S. H. Diks, K. Kok, T. O'Toole, D. W. Hommes, P. van Dijken, J. Joore, M. P. Peppelenbosch, J. Biol. Chem. 279 (2004) 49206-49213.

[7] S. A. Beausoleil, J. Villén, S. A. Gerber, J. Rush, S. P. Gygi, Nat. Biotechnol. 24 (2006) 1285-1292.

[8] Z. Wang, N. Sun, Y. He, Y. Liu, J. Li, Anal. Chem. 86 (2014) 6153-6159.

[9] M. G. Shapiro, J. O. Szablowski, R. Langer, A. Jasanoff, J. Am. Chem. Soc. 131 (2009) 2484-2486.

[10] C. Liu, L. Chang, H. Wang, J. Bai, W. Ren, Z. Li, Anal. Chem. 86 (2014) 6095-6102.

[11] D. L. Andrews, A. A. Demidov, Resonance energy transfer, Wiley, 1999.

[12] P. Carriba, G. Navarro, F. Ciruela, S. Ferre, V. Casado, L. Agnati, A. Cortes, J. Mallol, K. Fuxe, E. I. Canela, C. Lluis, R. Franco, Nat. Methods 5 (2008) 727-733.

[13] J. S. Lee, H.-A. Joung, M.-G. Kim, C. B. Park, ACS Nano 6 (2012) 2978-2983.

[14] C. Wang, Y. Tang, Y. Liu, Y. Guo, Anal. Chem. 86 (2014) 6433-6438.

[15] R. M. Clegg, Curr. Opin. Biotech. 6 (1995) 103-110.

[16] R. Freeman, T. Finder, R. Gill, I. Willner, Nano Lett. 10 (2010) 2192-2196.

[17] S. Xu, Y. Liu, T. Wang, J. Li, Anal. Chem. 83 (2011) 3817-3823.

[18] Y. Shan, J.-J. Xu, H.-Y. Chen, Chem. Commun. (2009) 905-907.

[19] H. Zhou, Y.-Y. Zhang, J. Liu, J.-J. Xu, H.-Y. Chen, J. Phys. Chem. C 116 (2012) 17773-17780.

[20] M.-S. Wu, H.-W. Shi, L.-J. He, J.-J. Xu, H.-Y. Chen, Anal. Chem. 84 (2012) 4207-4213.

[21] M.-S. Wu, H.-W. Shi, J.-J. Xu, H.-Y. Chen, Chem. Commun. 47 (2011) 7752-7754.

[22] C.-Y. Tian, W.-W. Zhao, J. Wang, J.-J. Xu, H.-Y. Chen, Analyst 137 (2012) 3070-3075.

[23] L. L. Li, J. Ji, R. Fei, C. Z. Wang, Q. Lu, J. R. Zhang, L. P. Jiang, J. J. Zhu, Adv. Funct. Mater. 22 (2012) 2971-2979.

[24] H.-F. Zhao, R.-P. Liang, J.-W. Wang, J.-D. Qiu, Chem. Commun. 51 (2015) 12669-12672.

[25] Q. Lu, W. Wei, Z. Zhou, Z. Zhou, Y. Zhang, S. Liu, Analyst 139 (2014) 2404-2410.

[26] R. Swathi, K. Sebastian, J. Chem. Sci. 121 (2009) 777-787.

[27] H. Dong, W. Gao, F. Yan, H. Ji, H. Ju, Anal. Chem. 82 (2010) 5511-5517.

[28] H. Zhao, Y. Chang, M. Liu, S. Gao, H. Yu, X. Quan, Chem. Commun. 49 (2013) 234-236.

[29] P. Wu, X. Hou, J.-J. Xu, H.-Y. Chen, Chem. Rev. 114 (2014) 11027-11059.

[30] D. Pan, J. Zhang, Z. Li, M. Wu, Adv. Mater. 22 (2010) 734-738.

[31] J. M. Bai, L. Zhang, R. P. Liang, J. D. Qiu, Chem-Eur. J. 19 (2013) 3822-3826.

[32] Y. Wang, L. Zhang, R.-P. Liang, J.-M. Bai, J.-D. Qiu, Anal. Chem. 85 (2013) 9148-9155.

[33] D. Li, M. B. Muller, S. Gilje, R. B. Kaner, G. G. Wallace, Nat. Nanotechnol. 3 (2008) 101-105.

[34] S.-M. Park, J.-S. Yoo, Anal. Chem. 75 (2003) 455 A-461 A.

[35] E. Han, L. Ding, H. Lian, H. Ju, Chem. Commun. 46 (2010) 5446-5448.

[36] X. He, Z. Chen, Y. Wang, K. Wang, J. Su, G. Yan, Biosens. Bioelectron. 35 (2012) 134-139.

[37] W. Song, Y. Wang, R.-P. Liang, L. Zhang, J.-D. Qiu, Biosens. Bioelectron. 64 (2015) 234-240.

[38] G. Cozza, P. Bonvini, E. Zorzi, G. Poletto, M.A. Pagano, S. Sarno, A. Donella-Deana, G. Zagotto, A. Rosolen, L.A. Pinna, F. Meggio, S. Moro, J. Med. Chem. 49 (2006) 2363-2366.

[39] S. Sarno, L. A. Pinna, Mol. BioSyst. 4 (2008) 889-894.

Figure Captions

Scheme 1. Illustration of ECL biosensor for monitoring CK2 activity and inhibitor screening.

Figure 1. TEM images of (A) GO and (B) GQDs. Inset of B: diameter distribution of GQDs. (C) FT-IR spectra of (a) GQDs and (b) carboxylated GQDs. (D) UV-vis absorption spectra of (a) GO, and PL spectra of (b) GQDs and (c) carboxylated GQDs. Inset of D: photographs of GQDs (1 and 2) and carboxylated GQDs (3 and 4) taken under visible light (1 and 3) and 365 nm UV light (2 and 4), respectively.

Figure 2. EIS of (a) bare electrode, (b) CS, (c) GQDs/CS, (d) peptide/GQDs/CS, (e) phosphorylated peptide/GQDs/CS modified electrodes, and (f) electrode (e) after assembly of Ab-GO. Inset: the equivalent circuit used to model the impedance data. Rs, solution resistance; Zw, Warburg diffusion resistance; Cdl, double-layer capacitance.

Figure 3. AFM images of (A) CS, (B) GQDs/CS, (C) peptide/GQDs/CS, and (D) Ab-GO/phosphorylated peptide/GQDs/CS films.

Figure 4. ECL-time curves of (a) bare electrode, (b) CS, (c) GQDs/CS, (d) peptide/GQDs/CS, and electrode (d) after assembly of Ab-GO in the presence of (e) 0 U/mL and (f) 5 U/mL CK2 and 50 μM ATP in 0.1 M PBS containing, 0.1 M KCl and 0.1 M $K_2S_2O_8$.

Figure 5. (A) ECL curves of the biosensor at different concentrations of CK2 (from a to j: 0, 0.05, 0.1, 1.0, 2.5, 5.0, 7.5, 10.0, 20.0 and 30.0 U/mL, respectively). (B) Relationship between the ECL_{GQDs} and the C_{CK2}. The detection was performed in 0.1 M pH 7.4 PBS containing 0.1 M KCl and 0.1 M $K_2S_2O_8$. Scan rate: 100 mV/s. Scan range: −1.6 V ~ 0 V.

Figure 6. (A) Relationship between ECL intensity and the different concentrations of ellagic acid. Inset: ECL intensity-time curves of the biosensor at different concentrations of ellagic acid. (B) The ECL intensity in the absence of inhibitor (control) and in the presence of 10 μM four different inhibitors (DRB, emodin, quercetin, and ellagic acid). The phosphorylation of peptide was carried out with 10 U/mL CK2 and 50 μM ATP.

Scheme 1

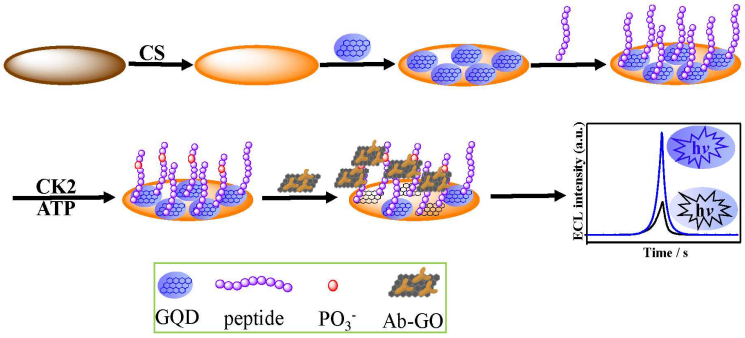

Figure 1

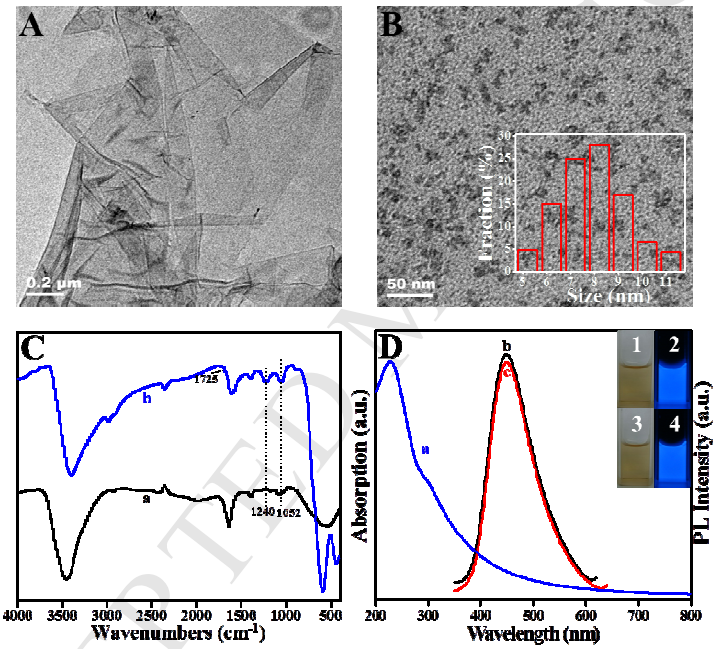

Figure 2

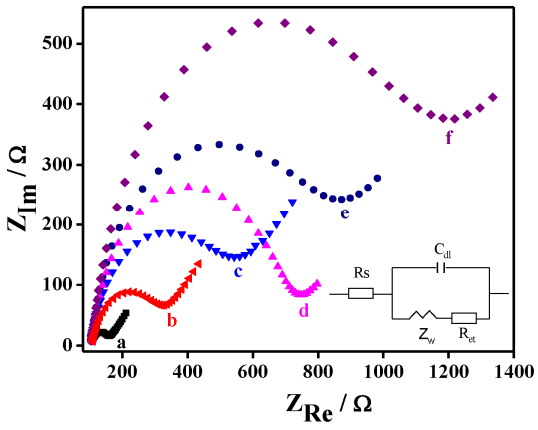

Figure 3

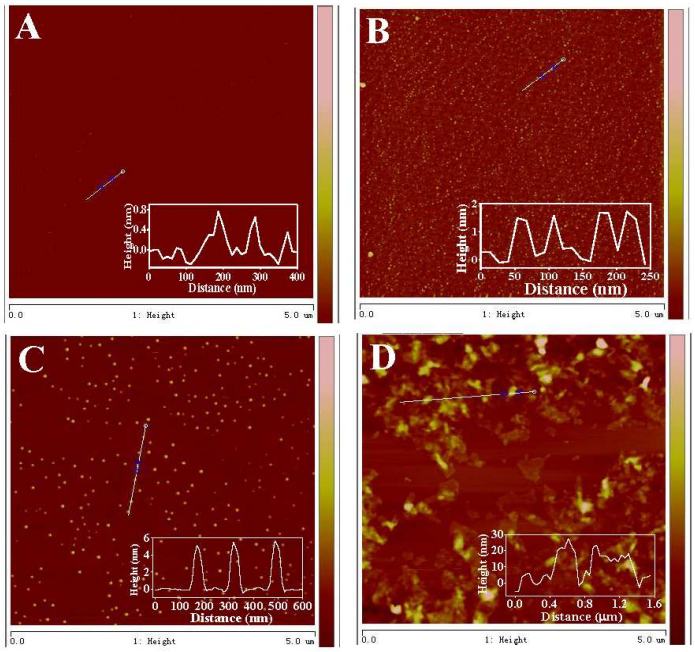

Figure 4

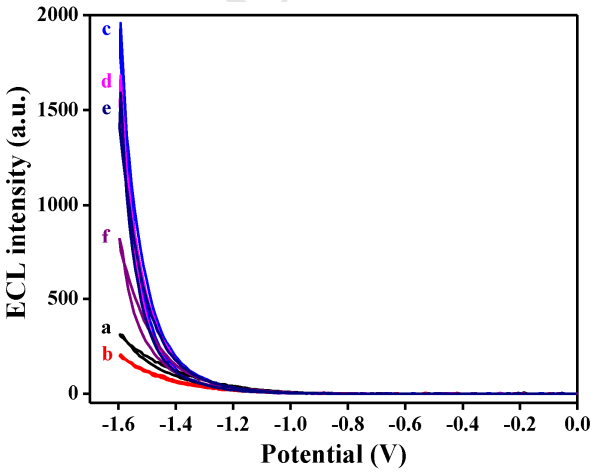

Figure 5

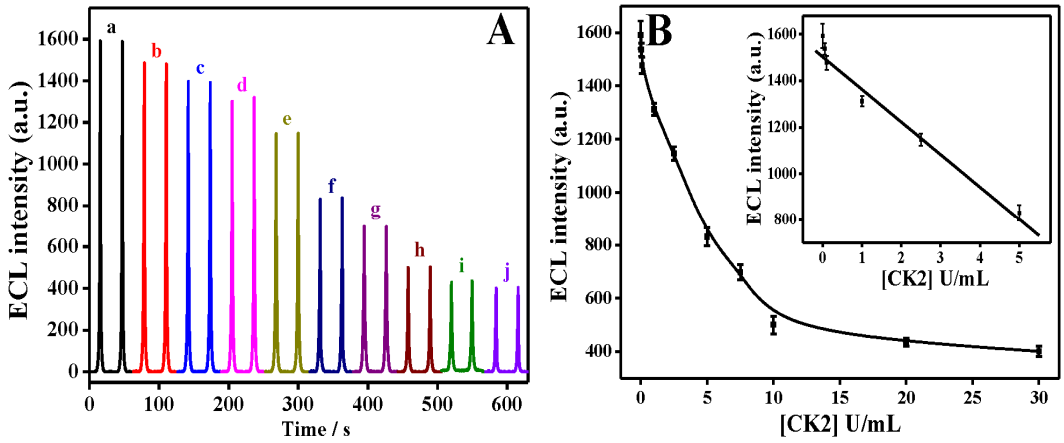

Figure 6

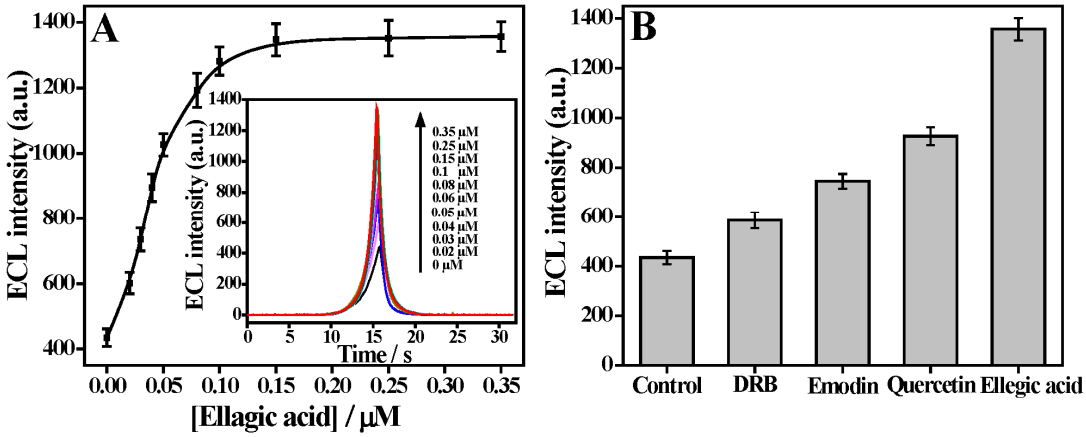

Highlights

- We reported a novel ECL-RET biosensor for sensitive analysis of casein kinase II activity.
- The successful ECL-RET between GQDs and GO could be established.
- GQDs was employed for casein kinase II activity monitoring and inhibition assay.
- Highly sensitive detection of CK2 activity and inhibition was achieved.